

Diversification, disparification and hybridization in the desert shrubs *Encelia*

Sonal Singhal¹ , Adam B. Roddy² , Christopher DiVittorio^{3,4}, Ary Sanchez-Amaya⁵, Claudia L. Henriquez⁵ , Craig R. Brodersen⁶ , Shannon Fehlberg⁷  and Felipe Zapata⁵ 

¹Department of Biology, CSU Dominguez Hills, 1000 E Victoria Street, Carson, CA 90747, USA; ²Institute of Environment, Department of Biological Sciences, Florida International University, Miami, FL 33133, USA; ³University of California Institute for México and the United States, University of California, 3324 Olmsted Hall, Riverside, CA 92521, USA; ⁴Pinecrest Research Corporation, 5627 Telegraph Avenue, Suite 420, Oakland, CA 94609, USA; ⁵Department of Ecology and Evolutionary Biology, University of California, 612 Charles E. Young Dr. South, Los Angeles, CA 90095, USA; ⁶School of the Environment, Yale University, New Haven, CT 06511, USA; ⁷Research, Conservation, and Collections, Desert Botanical Garden, 1201 N Galvin Parkway, Phoenix, AZ 85008, USA

Summary

Author for correspondence:
Sonal Singhal
Email: sonal.singhal1@gmail.com

Received: 31 July 2020
Accepted: 10 January 2021

New Phytologist (2021)
doi: 10.1111/nph.17212

Key words: aridity, deserts, *Encelia*, hybridization, phylogenomics, trait evolution.

- There are multiple hypotheses for the spectacular plant diversity found in deserts. We explore how different factors, including the roles of ecological opportunity and selection, promote diversification and disparification in *Encelia*, a lineage of woody plants in the deserts of the Americas.
- Using a nearly complete species-level phylogeny based on double-digest restriction-aided sequencing along with a broad set of phenotypic traits, we estimate divergence times and diversification rates, identify instances of hybridization, quantify trait disparity and assess phenotypic divergence across environmental gradients.
- We show that *Encelia* originated and diversified recently (mid-Pleistocene) and rapidly, with rates comparable to notable adaptive radiations in plants. *Encelia* probably originated in the hot deserts of North America, with subsequent diversification across steep environmental gradients. We uncover multiple instances of gene flow between species. The radiation of *Encelia* is characterized by fast rates of phenotypic evolution, trait lability and extreme disparity across environments and between species pairs with overlapping geographic ranges.
- *Encelia* exemplifies how interspecific gene flow in combination with high trait lability can enable exceptionally fast diversification and disparification across steep environmental gradients.

Introduction

Despite the seemingly barren landscape of arid habitats, desert ecosystems harbor some of the most spectacular plant evolutionary radiations (Klak *et al.*, 2004; Hernandez-Hernandez *et al.*, 2011). Why and how aridity has promoted the diversification of plant species and phenotypes has puzzled generations of ecologists and evolutionary biologists alike (Stebbins, 1952; Axelrod, 1972), resulting in several hypotheses. First, arid habitats worldwide began to form and expand only in the last 10 Myr (Arakaki *et al.*, 2011), a relatively short geological time-frame during which new regions of niche space became available. Additionally, deserts have been dynamic through space and time, with diverse orogenies, glacial cycles, marine incursions and volcanic eruptions that probably caused highly variable selection regimes, multiple cycles of migration–isolation, and eventually colonization and diversification in new habitats (Thompson & Anderson, 2000; Riddle *et al.*, 2000; Oskin & Stock, 2003; Conly *et al.*, 2005). Second, in deserts, substantial topographic, edaphic,

climatic and ecological heterogeneity results in a diversity of habitats, across which species can persist and diversify (Ellis *et al.*, 2006; Sosa *et al.*, 2020). Third, the environmental factors that characterize arid ecosystems typically represent extreme conditions for plant functioning and survival, including, but not limited to, drought stress, high UV radiation, high temperature and high salinity (Sandquist, 2014). These extreme conditions often occur over narrow geographic regions. When these multiple stressors converge, multiple, functionally equivalent solutions to the same challenge can evolve. This can lead to phenotypic disparification in otherwise seemingly homogeneous environments (Niklas, 1994).

The confluence of these geological, environmental and ecological factors in arid ecosystems are probably crucial in spurring the radiation of resident plant lineages (Hernández-Hernández *et al.*, 2014; Said Gutiérrez-Ortega *et al.*, 2018), and the multiplicity of strong selective agents that occur in arid ecosystems may be responsible for the remarkable morphological and physiological diversity that have evolved among desert plants. Desert lineages,

therefore, provide ideal case studies of the role of selection in plant radiations. Yet, studies that link the evolutionary history of a lineage with patterns of phenotypic, ecological, climatic and environmental variation are lacking, and thus our understanding of the processes of diversification of plants in arid regions remains elusive. Here, we use an integrative approach to document the evolutionary radiation of shrubs in the genus *Encelia* (Asteraceae), which are widespread throughout the deserts of the Americas, and showcase how multiple factors – abiotic, biogeographic, phenotypic and population dynamics – interact to produce high diversification within a clade.

Most species of *Encelia* are distributed in the arid lands of southwestern North America, the dry lands of Chile, Peru and Argentina, and the (arid) Galapagos Islands (Clark, 1998). These plants inhabit various types of desert, including inland deserts, coastal dunes, as well as high and low deserts; *E. actoni* even passes the frost line in the Sierra Nevada mountain range of California. Given the widespread distribution of *Encelia*, it is plausible that the dynamic geologic and climatic history of the arid habitats has provided multiple opportunities for lineage separation and diversification (Spotila *et al.*, 1998; Dolby *et al.*, 2015). Indeed, previous work has shown that range fragmentation and expansion associated with climatic changes during the Pleistocene have influenced the spatial distribution of genetic diversity in the widespread *Encelia farinosa* (Fehlberg & Ranker, 2009; Fehlberg & Fehlberg, 2017). However, the influence of biogeographic, ecological or other abiotic forces on the radiation of the genus *Encelia* is unknown.

Commonly referred to as brittlebushes, *Encelia* species display remarkable ecophenotypic diversity, and their phenotypic traits are strongly associated with habitat differentiation (Ehleringer & Clark, 1988; Clark, 1998). The species range from small to medium-sized shrubs (0.2–1.5 m in height) but exhibit substantial variation in overall plant architecture. Leaf morphology is exceptionally diverse in *Encelia*. The leaves are always simple and spirally arranged but vary extensively in shape, margin, size and indumentum. Classic studies in plant ecophysiology have shown fitness tradeoffs between leaf morphological traits and physiological functions that are associated with fine-scale habitat differentiation (Ehleringer *et al.*, 1981; Ehleringer, 1988). In contrast to vegetative structures, inflorescence morphology, floret morphology and flowering phenology in *Encelia* do not display substantial diversity, consistent with Asteraceae more generally. Thus, much of the phenotypic diversification in *Encelia* occurs among vegetative structures, although the overall tempo and mode of phenotypic evolution – including the rate of trait evolution and correlation in evolution across traits – in *Encelia* is not understood.

As currently circumscribed, *Encelia* includes 15 species and five subspecies (Clark, 1998). Most species are allo- or parapatric, but contact zones where natural hybrids form are common throughout the geographic range of *Encelia* (Clark, 1998). Natural hybridization is rampant in *Encelia* (Kyhos, 1967; Kyhos *et al.*, 1981), and some species are hypothesized to result from hybrid speciation (Allan *et al.*, 1997). Nevertheless, all species seemingly maintain their phenotypic cohesion and independence. Although

divergent selection can maintain species despite widespread hybridization (DiVittorio *et al.*, 2020), whether interspecific gene flow increases genetic diversity through hybridization or introgression among *Encelia* species and thus enables lineages to take advantage of new ecological opportunities is not known.

Understanding the evolution of the unique ecology, phenotypic diversity and the role of gene flow in the radiation of *Encelia* require a well-resolved phylogeny of the group. Variation in morphology, secondary chemistry and sequence data show that *Encelia* is monophyletic and most closely related to *Geraea* and *Enceliopsis*, both of which consist of arid-adapted, perennial herbs. However, the relationships among *Encelia* species have been difficult to resolve (Clark, 1998; Fehlberg & Ranker, 2007). Here we present a broadly sampled phylogenetic analysis of *Encelia* using RADseq from 12 *Encelia* species and two outgroup species. Using this phylogeny, we address four questions: what is the evolutionary history of *Encelia*; what is the tempo and mode of diversification and trait disparification in *Encelia*; what are the main drivers of diversification and trait disparification in *Encelia*; and what is the role of interspecific gene flow in this evolutionary radiation?

Materials and Methods

Here, we briefly summarize our approach for sampling, genetic data collection and analysis, and trait and spatial data collection and analysis. Full details are available in the Supporting Information Methods S1.

Sampling

We sampled trait and genetic data from 12 of the 15 recognized species in *Encelia* (Fig. 1; Tables S1, S2). Where possible, we collected individuals across the range. For all species, we collected leaf and seed material during field seasons ranging from 2009 to 2016. Species were grown in a common garden at the University of California Agricultural Operations Station (Riverside, CA, USA). Phenotypic measurements and tissues for genetic analysis were taken from adult individuals in the garden for all species but *Encelia ravenii* and *Encelia resinifera*, for which we used field-collected adult leaves.

Genetic data collection

We collected genetic data using double-digest restriction-aided (ddRAD) sequencing for 77 individuals. We first extracted DNA from silica-dried adult leaves and then prepared doubly barcoded ddRAD libraries (Peterson *et al.*, 2012) using *Pst*I and *Msp*I and size-selecting fragments from 250 to 700 bp. All libraries were pooled and sequenced across one lane of 100 paired-end sequencing on the Illumina HiSeq 4000 Sequencing Platform.

To process and analyze these data, we wrote a pipeline that generates both pseudoreference genomes per lineage and variant call sets across individuals within a lineage. Because this approach generates a common reference index across lineages, it is easier to identify homologous loci and variants. First, we cleaned and

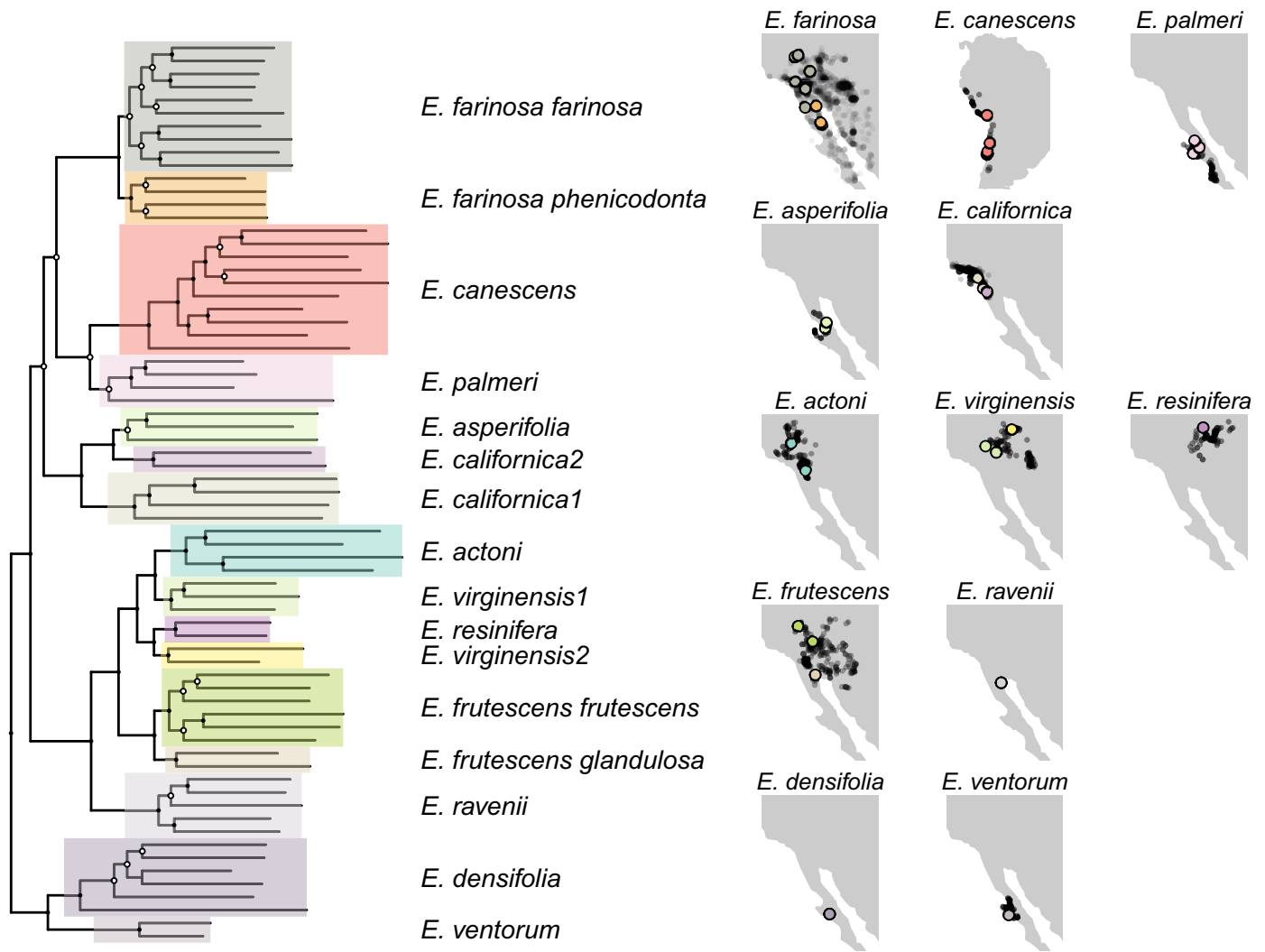


Fig. 1 Individual-level phylogeny of *Encelia*, inferred using RAxML on a concatenated alignment of 31 000 loci. Shaded boxes demarcate lineage-level clades; nodes with bootstrap < 95% are indicated in white. Maps show distribution of nominal species based on Global Biodiversity Information Facility (GBIF) data as light gray points. Large filled points indicate sampling locations for individuals used in this study, colored by lineage identity.

assembled reads using TRIMMOMATIC v.36 (Bolger *et al.*, 2014), PEAR v.0.9.8 (Zhang *et al.*, 2014), and VELVET v.1.2.10 (Zerbino & Birney, 2008). Second, we determined lineage identity per individual. Although all sampled individuals were identified to nominal species, species boundaries have not been well tested in *Encelia*. After identifying homologous loci across individuals using VSEARCH v.2.9.1 (Rognes *et al.*, 2016), we inferred an individual-level phylogeny using RAxML v.8.2.11 on an 11 600 loci, 1.5 Mb concatenated alignment (Stamatakis, 2014). By comparing clade identity with nominal species identity, we determined likely lineage identities for each individual (Table S1). Finally, we generated a pseudoreference genome per lineage using an iterative reference-based approach (Sarver *et al.*, 2017). Across all individuals, we generated an initial pseudoreference genome by selecting the longest locus for each of 244 000 homolog groups. Per lineage, we mapped reads to the starting pseudoreference genome using BWA v.0.7.17 (Li, 2013), called variants using SAMTOOLS v.1.5 (Li *et al.*, 2009), and then mutated the current

pseudoreference genome to incorporate any variants at $\geq 50\%$ allele frequency. This was repeated three additional times. We generated the final variant set per lineage by using BWA to align reads and then calling genotypes using SAMTOOLS. We retained all sites with quality scores > 20 and depth $\geq 10\times$.

Genetic data analyses

Phylogenetic inference Given the potential challenges of phylogenetic inference with ddRAD data (DaCosta & Sorenson, 2016 but see Eaton *et al.*, 2017), we compared topologies across both concatenated and coalescent-based methods for phylogenetic inference. For an individual-level phylogeny, we used RAxML to infer a phylogeny and 100 bootstrap replicates from a 31 000 loci, 3.9 Mb concatenated alignment. We used SVDQUARTETS based on 2800 single nucleotide polymorphisms (SNPs) to infer a coalescent-based phylogeny with 100 bootstrap replicates (Chifman & Kubatko, 2014). Additionally, we calculated gene

concordance factors (gCFs) and site concordance factors (sCFs) using IQ-TREE v.1.6.4 (Minh *et al.*, 2020), to assess conflict across loci and sites.

For a lineage-level phylogeny, we used two coalescent-based approaches. First, we filtered our alignment to retain those with <40% missing data, inferred gene trees inferred using RAxML, and then used ASTRAL-III (Zhang *et al.*, 2018) to infer a species tree based on these 29000 gene trees. We repeated this analysis with gene tree sets of <30% and <20% missing data to confirm that amounts of missing data did not affect inference. Second, we used SVDQUARTETS with the same SNP dataset used for the individual-level SVDQUARTETS phylogeny (see earlier). To infer a time-calibrated phylogeny, we first used RAxML to estimate branch lengths based on a concatenated alignment on a constrained topology inferred with Astral-III. Then, we used an external calibration from a comprehensive angiosperm phylogeny that estimated the crown age of *Encelia* as 1.36 Myr (Magallón *et al.*, 2015; Smith & Brown, 2018). This aligns with previous divergence dating based on population genomic data that inferred the crown of *Encelia* as 1.05 Myr (S. Singhal, unpublished). We used this root age to infer a chronogram using the 'chronos' function in the R package APE under a strict clock model with a λ of 0. We selected our model and λ -value by comparing Φ IC across all possible models and a range of λ -values from $1e-6$ to 0.1 (Fig. S1; Paradis, 2013). We used this time-calibrated phylogeny in all comparative analyses.

Introgression Given that previous analyses and field studies have suggested hybridization is common in *Encelia* (Clark & Allan, 1997; Allan *et al.*, 1997), we used two complementary approaches to identify likely instances of historical and current introgression. First, we inferred phylogenetic networks using SNAQ v.0.9.0 (Solís-Lemus & Ané, 2016). As input, we provided gene trees, removing any gene trees with >50% missing data. We then ran SNAQ for zero to five reticulate edges, for three independent replicates each, using the ASTRAL tree as the starting topology. Second, we calculated the D-statistic across lineages, which quantifies when topological variance is in excess of what would be predicted under incomplete lineage sorting (Durand *et al.*, 2011). In contrast to SNAQ, which performs best when reticulation edges occur between more distantly related lineages (Solís-Lemus & Ané, 2016), the D-statistic compares close relatives. Using all possible species triads based on the ASTRAL topology with *Enceliopsis covelli* as the outgroup, we calculated an allele frequency-based D-statistic. We then calculated significance of the D-statistic by conducting 1000 bootstraps and calculating the Z-score (Eaton & Ree, 2013). For a given species pair, we report the D-statistic calculated using the nearest neighbor as the third lineage. If this still resulted in multiple comparisons, we conservatively report the D-statistic with the smallest Z-score (Malinsky *et al.*, 2018).

Trait data collection

We collected nine morphological and physiological traits (summarized in Table S3) to determine the extent and nature of phenotypic variation. Where possible, we sampled multiple individuals per species (Table S2).

Leaf area, shape and color To analyze leaf area, shape, and color, we collected and photographed three to five adult leaves per individual growing in the common garden. We analyzed leaf images using IMAGEJ (Abràmoff *et al.*, 2004). To measure color, we used the white-balanced leaf images in Adobe PHOTOSHOP and measured the arithmetic mean of all pixels of the largest circumscribed rectangle possible within the center of the leaf. Leaf mass was measured on dry leaves and used to calculate leaf mass per area (LMA).

Canopy ramification and wood density We estimated the degree of canopy ramification as the number of terminal branch tips per stem cross-sectional area (BTSA; Roddy *et al.*, 2019) on plants growing in the common garden. Wood density of stems stripped of their bark was measured using Archimedes' principle by measuring the mass of water displaced on a balance and subsequently measuring the dry mass of the stems.

Stem hydraulic conductance Whole-shoot hydraulic conductance was measured using a low-pressure flow meter (Kolb *et al.*, 1996), which enables measurement of the entire shoot regardless of branch ramification and can be applied to morphologically diverse structures (Roddy *et al.*, 2016, 2019). Measurements were taken on healthy shoots from well-watered and mature plants. Hydraulic conductance was calculated as the slope of the regression of flow rate versus pressure. Because shoots differed in size and ramification, hydraulic conductance was normalized by leaf area of the shoot, which is taken as a metric of hydraulic efficiency (Roddy *et al.*, 2019).

MicroCT imaging High-resolution, three-dimensional (3D) images of stem and leaf structure were obtained by performing hard X-ray microcomputed tomography (microCT) at the Advanced Light Source, Lawrence Berkeley National Laboratory (LBNL), Beamline 8.3.2 (Brodersen, 2013; Brodersen & Roddy, 2016). Mature leaves and stems were sampled from plants growing in the common garden and imaged within 48 h. Stems were allowed to air-dry before microCT imaging to ensure that vessels had emptied, and leaves were kept sealed in moist plastic bags until immediately before imaging.

To characterize trichome density, digital slices parallel to the fresh leaf surface were taken through the trichomes, allowing trichomes to be counted per unit projected leaf surface area. Stem xylem vessel diameter and area were measured using IMAGEJ on two-dimensional cross-sections of microCT image stacks obtained from dried stems.

Spatial data collection

To determine the geographic extent and climatic envelope of *Encelia* species, we downloaded all occurrence data for *Encelia* species from the Global Biodiversity Information Facility (GBIF) on 10 June 2019 (GBIF, 2019). Using the R package COORDINATECLEANER (Zizka *et al.*, 2019), we removed points falling in the ocean and retained only those points from preserved specimens or human observations. By species, we then removed

extreme spatial outliers using the 'cc_outl' function, removed duplicate records, and thinned data by 1 km using the R package SPThin (Aiello-Lammens *et al.*, 2015).

Using these cleaned and thinned data, we extracted climatic and soil data using WorldClim 2.0 rasters at 30 s resolution (Fick & Hijmans, 2017) and the Unified North American Soil Map at 0.25 degree resolution (Liu *et al.*, 2014). For climatic data, we focused on four bioclimatic variables that reflect extreme climatic conditions and are likely to be important in determining plant survival: maximum temperature of the warmest month (bioclim 5), minimum temperature of the coldest month (bioclim 6), precipitation of the wettest month (bioclim 13), and precipitation of the driest month (bioclim 14). We summarized the 18 soil variables describing soil composition and acidity using a principal component analysis (PCA) and retained the first two axes that explained 22% and 19% of the variation in total. All spatial analyses were conducted using the R packages RASTER and RGEOS (Hijmans *et al.*, 2015; Bivand & Rundel, 2017).

Comparative analyses

To determine net diversification rate, we used the crown age estimator across a range of extinction rates and our time-calibrated phylogeny (Magallón & Sanderson, 2001). We explored three scenarios for extinction ($\epsilon = 0.1, 0.3$ and 0.9); the parameter ϵ reflects the balance between speciation and extinction rates.

To characterize the tempo and mode of trait evolution, we used species-level means and estimated phylogenetic signal (λ) for each trait (Pagel, 1999). In addition, we calculated the rate of trait evolution using *felsens*, a metric that quantifies the increase in the variance through time in trait values among sister taxa (Ackerly, 2009). To measure correlations between traits and correlations between traits and environmental variables, we first conducted a phylogenetic canonical correlation analysis (Revell & Harrison, 2008). We then conducted more targeted correlation tests using phylogenetic generalized least squares, using a Brownian motion correlation matrix. We used the R packages PHYTOOLS, GEIGER, APE, NLME and GGTREE to conduct and visualize all comparative analyses (Paradis *et al.*, 2004; Harmon *et al.*, 2008; Pinheiro, 2009; Revell, 2012; Yu *et al.*, 2017).

To determine the biogeographic history of *Encelia*, we used BIOGEOBEARS (Matzke, 2013) to estimate ancestral ranges. Occurrence data were mapped onto Ecological Regions of North America (Omernik & Griffith, 2014) to assign extant species to one or more of six biogeographic areas: Baja California Deserts, Mediterranean, Mojave Desert, Sonoran Desert, the cold deserts, or Peru (Fig. S2). We ran the dispersal–extinction–cladogenesis (DEC) only, given limitations of more complex models (Ree & Sanmartín, 2018). We set the maximum possible range size to four.

We compared how species pairs have diverged across environmental and morphological variables. For each of the morphological, soil and climatic datasets, we first summarized the data using a scaled and centered PCA. For the first PC axis for each dataset, we calculated divergence between species as the Euclidean distances between species-level means. For each pairwise

comparison, we also determined geographic range overlap. We first inferred species geographic range based on the alpha convex hull of occurrence data and then estimated overlap in convex hulls (Pateiro López & Rodríguez, 2010). Following the approach outlined by Weber *et al.* (2018), for each species pair and each measure of trait divergence (e.g. morphology, soil or distance), we calculated the rate of divergence by dividing trait divergence by phylogenetic distance. We then compared the mean rate of divergence between allopatric and sympatric species pairs. To determine if the comparison was statistically significant, we generated a distribution using 1000 simulations of each trait under Brownian motion. In each simulation, we kept sympatric and allopatric designations fixed and then calculated the rate of divergence.

Results

Genetic data analyses

After dropping five individuals that yielded < 5% of homologous loci, our final dataset resulted in an average of 870 Mb sequence across an average of 60 000 loci for 72 individuals (Table S1). Using these genetic data, we first determined likely lineage assignments among all sampled individuals, finding evidence of non-monophyly of *E. californica* and *E. virginensis* (Fig. S3). We accordingly revised lineage designations in these two nominal species to reflect the presence of putative new lineages (Table S1). The individual-level phylogeny based on these new lineage designations recovers the same topology as the lineage-level phylogeny (Figs 1, 2) and the coalescent-based and concatenated phylogeny are largely concordant at the interspecific level (Fig. S3). The individual-level phylogeny exhibits high bootstrap support for the monophyly of all lineages but *E. palmeri* and *E. asperifolia* (Figs 1, S4). However, sCF and gCF are low compared with bootstrap support (Fig. S4), which might be expected given that internode distances in our phylogeny are short and that the loci used to infer gene trees were short.

Despite the potential challenges of phylogenetic inference with ddRAD data – including the effects of missing data and the limitations of short loci – our phylogenetic reconstruction of lineage-level relationships was robust across inference method and amounts of missing data (Figs S5, S6). These phylogenies recovered three major clades (Fig. 2), two of which had been previously characterized as the *californica* and *frutescens* clades based on the species comprising the clades (Ehleringer & Clark, 1988; Fehlbeg & Ranker, 2007). Additionally, we identified a third clade consisting of *E. densifolia* and *E. ventorum*. In contrast to previous phylogenetic studies for *Encelia*, statistical support for all nodes was uniformly high except for the placement of *E. farinosa* (local posterior probability = 0.93).

Phylogenetic networks inferred by SNAQ strongly supported one hybridization edge between *E. californica* 2 and *E. asperifolia*, with admixture proportions of 0.49 and 0.51 between the two species (Fig. S7). Our *D*-statistic results identified multiple, strongly supported examples of introgression among lineages (Fig. S8; Table S4).

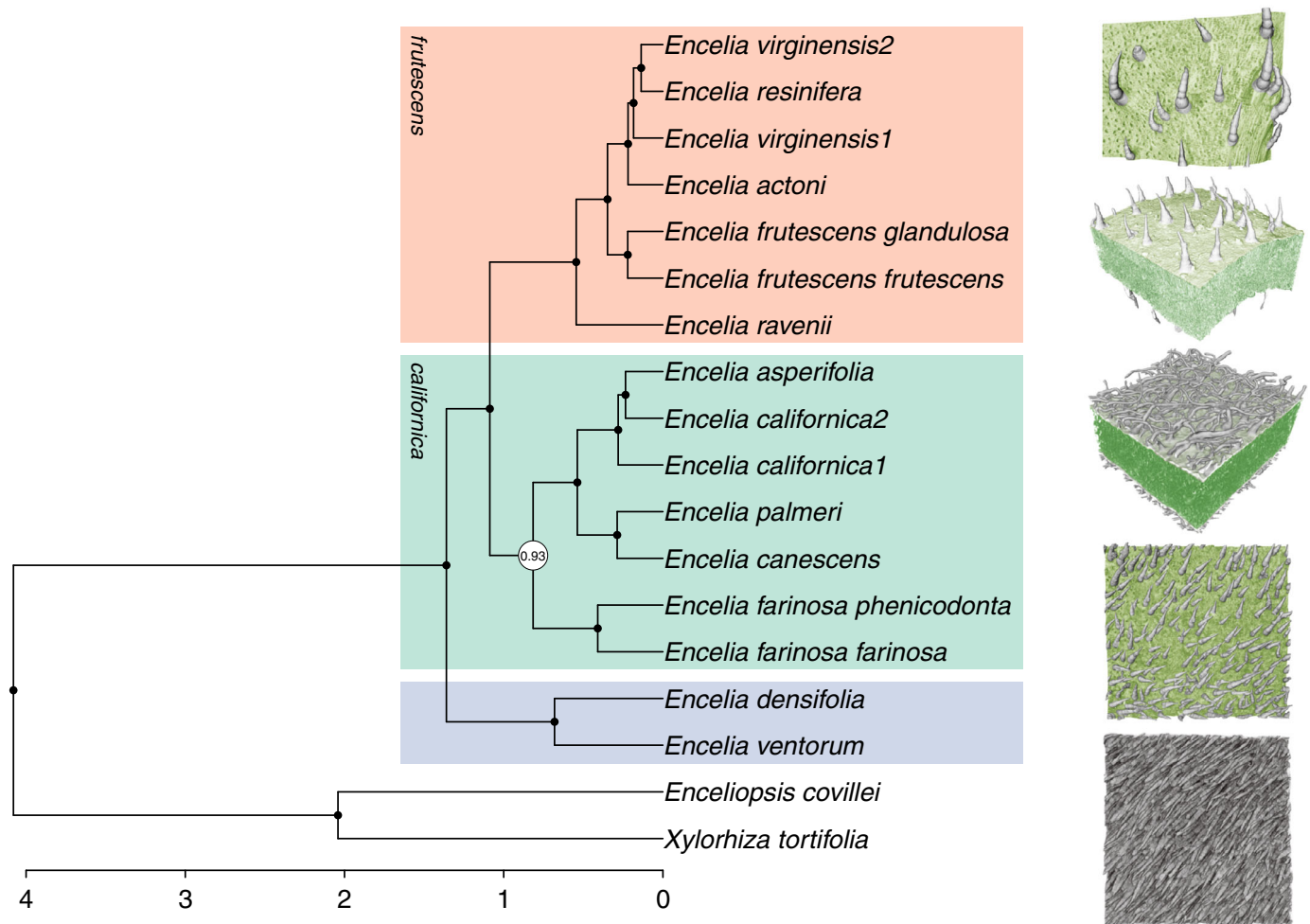


Fig. 2 A lineage-level *Encelia* phylogeny inferred using the coalescent-based approach ASTRAL-III. Microcomputed tomography images show external leaf morphology of the following (top to bottom, with approximate widths of leading edges in parentheses): *E. frutescens frutescens* (950 μm), *E. asperifolia* (550 μm), *E. palmeri* (650 μm), *E. densifolia* (950 μm) and *Enceliopsis covillei* (475 μm). Images were false-colored to indicate green photosynthetic tissue and how trichomes alter leaf color. Boxes demarcate major clades; timescale is shown in Myr. Nodes with < 95% local posterior probability are shown in white.

Comparative analyses

Using the crown age estimator across a range of extinction rates and our time-calibrated phylogeny (Fig. 2), we found that rates of diversification in *Encelia* vary from 1.57 ($\epsilon = 0.1$), to 1.52 ($\epsilon = 0.3$), to 0.66 species Myr^{-1} ($\epsilon = 0.9$) depending on the extinction scenario.

Reconstruction of trait evolution showed that closely related species often have divergent trait values, indicative of widespread phenotypic divergence among *Encelia* species (Figs 3, S9). This pattern of trait divergence is reflected in both low phylogenetic signal across all traits tested except leaf area (average $\lambda = 0.19$, range: 0–1.12; Table 1) and rapid trait evolution (average $\text{felsen} = 1.32$, range: 0.02–9.26; Table 1). Rapid evolution in traits is mirrored by rapid transitions in environmental space in *Encelia*. Both within and among species and clades, a wide diversity of climatic space is occupied (Figs S9, S10) and closely related species often occupy very distinct climatic spaces (Figs 3,

S9). For example, individual species or clades can occupy temperatures from below freezing to $> 40^\circ\text{C}$ or rainfall from close to 0 mm to 200 mm (Figs 3, S9).

Correlations between traits were generally weak, and only a few trait correlations were significant (Fig. S11). Our phylogenetic canonical correlation analysis found no significant correlations between trait and environmental axes (Table S5). Further, very few of the comparisons between traits and environmental variables were significant (Fig. S12), even though most correlations followed general physiological predictions (Table S6).

The ancestral range reconstruction under DEC in BIOGEOBEARS returned fairly uncertain inference at deeper nodes. However, these results confirmed the origins of *Encelia* in some combination of the hot deserts (e.g., the Sonoran, Baja and Mojave Deserts; Fig. S1).

Sympatric species show a greater rate of climatic divergence from allopatric species, although this difference is not statistically

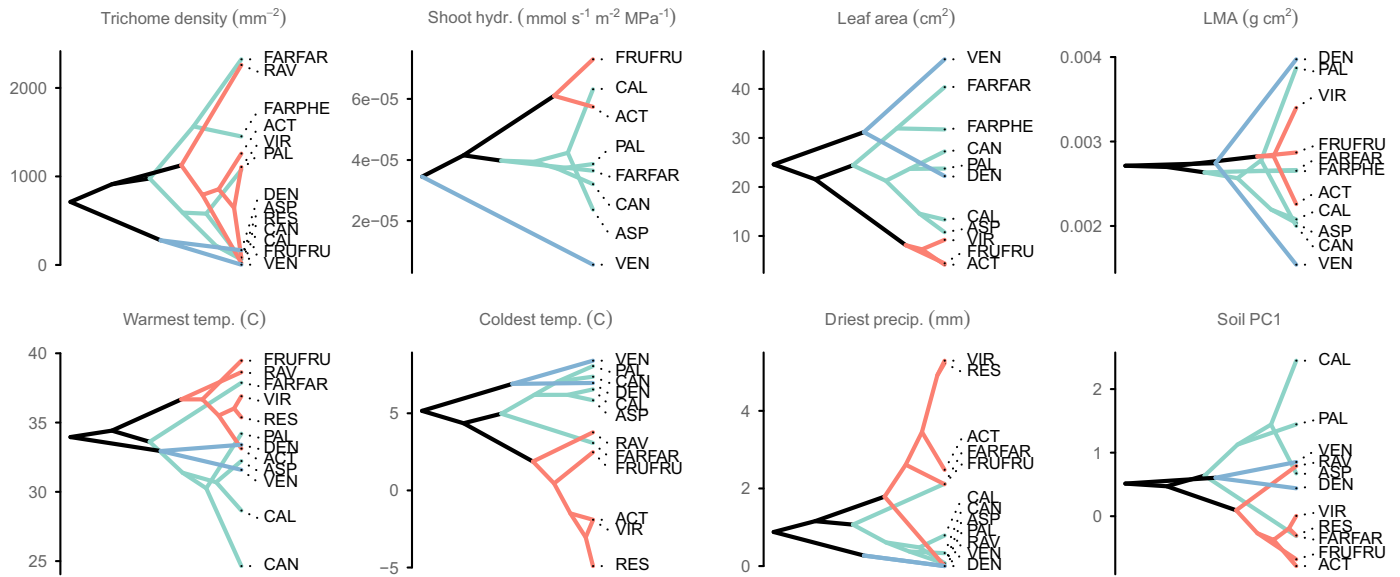


Fig. 3 Phenotypic variation in *Encelia* depicted as phenograms. The y-axis indicates phenotypic spread across (top) morphological and physiological traits and (bottom) environmental space. All climatic variables are the extreme values across months. Branches are colored by clade identity as shown in Fig. 2, and all species names are abbreviated to the first three characters. Data for additional traits and environmental measures are shown in Supporting Information Fig. S9. Closely related species in *Encelia* often exhibit dramatically different phenotypes. LMA, leaf mass area.

Table 1 Estimates of phylogenetic signal (λ) and the associated significance and evolutionary rates (felsen; β) for each of the nine measured morphological and physiological traits in *Encelia*.

Traits	λ	P-value	β	No. of tips
Canopy ramification (BTSA)	0	1	1.15	13
Trichome density (top)	0	1	9.26	15
Stem hydraulic conductance	0.43	0.81	0.61	8
Leaf color	0.18	0.79	0.03	11
Leaf area	1.12	0.01	0.55	11
Leaf roundness	0	1	0.05	11
Leaf mass area (LMA)	0	1	0.19	11
Wood density	0	1	0.02	5
Vessel diameter	0	1	0.09	11

BTSA, number of terminal branch tips per stem cross-sectional area.

significant ($\mu_{\text{sym-allo}} = 1.23$, $P = 0.06$; after removing outlier, $\mu_{\text{sym-allo}} = 0.41$, $P = 0.53$). By contrast, allopatric species show a greater rate of soil divergence than sympatric species ($\mu_{\text{sym-allo}} = -0.26$, $P = 0.02$; after removing outlier, $\mu_{\text{sym-allo}} = -0.97$, $P = 0$). Finally, sympatric species show a greater rate of morphological divergence than allopatric species ($\mu_{\text{sym-allo}} = 0.22$, $P = 0.041$; Fig. 4). The outlier in both the climate and soil divergence stems from a comparison of *E. resinifera* and *E. virginensis*, two closely related putative hybrid species that both live in the cold deserts.

Discussion

Encelia is an enigmatic but charismatic group that has been a model system for ecophysiological studies of desert plants (Ehleringer *et al.*, 1981; Ehleringer, 1988; Ehleringer & Cook,

1990; Ehleringer & Sandquist, 2018). Because the radiation of *Encelia* was recent, rapid and marked by introgression, previous phylogenetic studies based on both molecular and phenotypic data have failed to infer a well-resolved phylogeny of this genus (Fehlberg & Ranker, 2007). Aided by a phylogenomic dataset and extensive taxon sampling, we disentangled this radiation and resolved the evolutionary relationships among all sampled species (Fig. 2). In particular, we inferred the relationships between and within two previously identified clades: the *frutescens* clade, which includes the species found in the cold deserts of North America (*E. actoni*, *E. virginensis*, *E. resinifera*, *E. frutescens* and *E. ravenii*); and the *californica* clade, which includes the majority of the diversity found in Baja California (*E. farinosa*, *E. canescens*, *E. palmeri*, *E. asperifolia* and *E. californica*). Further, we found support for a new clade including *E. densifolia* and *E. ventorum*, both species restricted to Baja California. Together, these results suggest a pattern of phylogenetic ecogeographic structure whereby closely related species are largely restricted to the same or adjacent ecogeographic region (Figs 1, S2).

Rapid recent diversification and disparification in *Encelia*

Encelia has diversified recently and rapidly (Fig. 2), with 0.9–1.57 species produced per Myr. In comparison, Hawaiian silverswords radiated at 0.56 species Myr⁻¹ (Baldwin & Sanderson, 1998), Southern African ice plants at 0.77–1.75 species Myr⁻¹ (Klak *et al.*, 2004), and New World *Lupinus* at 2.49–3.79 species Myr⁻¹ (Hughes & Eastwood, 2006). Further, the two genera most closely related to *Encelia* (*Enceliopsis* and *Geraea*) are both relatively species-poor (four and two species, respectively), have older crown ages (Smith & Brown, 2018), and, accordingly, have much lower diversification rates. Thus, both within its local

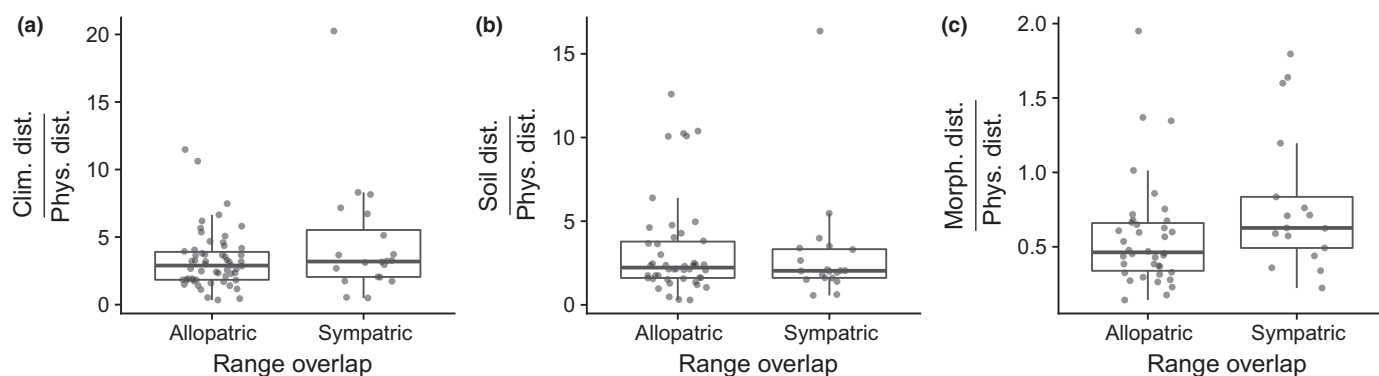


Fig. 4 (a–c) Rates of divergence between allopatric and sympatric species pairs in *Encelia* for climate (a), soil (b) and morphology (c). Boxes and the bisecting line reflect the interquartile range and the median, respectively. Whiskers reflect the largest and smallest values within $1.5 \times$ interquartile range. All data are plotted as gray dots with jitter for ease in visualization. Differences in rates of divergence are nonsignificant for climate (clim.), significantly lower in sympatric species for soil, and significantly higher in sympatric species for morphology (morph.). These results suggest that morphological divergence between sympatric species is greater than would be expected given the age of these species. dist., distance.

phylogenetic context and compared with other plant groups, *Encelia* has relatively high rates of diversification.

Concomitant with rapid diversification, *Encelia* shows rapid disparification. The absolute range of phenotypes seen within *Encelia* is broad even between closely related species, with leaf area varying 10-fold and trichome density varying > 1000 -fold (Figs 3, S9). While this range is narrow relative to the full diversity seen in angiosperms (Wright *et al.*, 2004), it is striking given the young age of *Encelia*. Accordingly, *Encelia* has rates of trait evolution comparable to notable adaptive radiations. For example, leaf size evolves at an estimated 0.55 felsen vs 0.46 in lobeliads and 2.08 in silverswords (Table 1; Ackerly, 2009). Unfortunately, we lack comparative data from other plant radiations for many of the traits we measured in *Encelia*. However, our estimated rates of evolution for other traits are high, exhibiting felsen > 5 for trichome density, even without accounting for the multiple types of trichomes that occur among *Encelia* (Fig. 2; Ehleringer & Cook, 1987).

Although closely related species diverge extensively in phenotype, distantly related species often share similar phenotypes (e.g., *E. farinosa farinosa* and *E. ravenii* in trichome density; Fig. 3). This pattern of low phylogenetic signal suggests that accessibility to adaptive traits has enabled *Encelia* to diversify across a mosaic of environmental conditions and adaptive optima. Along with rapid trait evolution, closely-related *Encelia* species often exist in very different climate and soil gradients (Figs 3, S9, S10). This pattern suggests that *Encelia* species are capable of rapidly adapting to novel environmental conditions. Taken together, our findings suggest that high trait lability and rapid trait evolution are key syndromes underpinning the evolvability of the *Encelia* radiation.

Drivers of diversification and disparification in *Encelia*

Encelia represents an excellent system for testing hypotheses regarding why deserts can generate exceptional diversity. First, the recent formation of arid habitats has provided new habitats in which desert-adapted species can diversify (Mooney & Zavaleta, 2016; Wang *et al.*, 2018). Indeed, although reconstruction of

Encelia's ancestral ranges was inconclusive, it suggested that *Encelia* most likely originated in the hot deserts, from which the *frutescens* clade spread into the cold deserts *c.* 0.5 Myr (Fig. S1). Outside of the two species (*E. canescens* and *E. hispida*) that colonized Peru and the Galapagos Islands, the center of biodiversity of *Encelia* is in the deserts of North America. These deserts have changed through time and across space over the last 5 Myr, with their initial formation and subsequent volcanic eruptions that likely eradicated much of the living flora (Conly *et al.*, 2005; Garrick *et al.*, 2009), sea incursions that divided the peninsula into isolated landmasses (Holt *et al.*, 2000; Riddle *et al.*, 2000), tectonic movement that led to the creation of the Baja peninsula (Dolby *et al.*, 2015), and glacial climate cycles that affected sea levels and habitat distributions (Van Devender & Spaulding, 1979; Thompson & Anderson, 2000). These landscape changes fall within the time-frame of the evolutionary history of *Encelia*, as it diverged from its sister lineages (stem age *c.* 4 Myr; Fig. 2) to the radiation of its extant species (crown age *c.* 1.4 Myr; Fig. 2). These changes both allowed colonization of new habitats and divided existing populations, resulting in population isolation that would lead to increased diversification. Indeed, the population structure of multiple animal and plant species in the North American deserts (Riddle *et al.*, 2000; Crews & Hedin, 2006; Garrick *et al.*, 2009) reflects this history, most notably with splits across northern and southern Baja California and across the Sonoran and Baja Californian deserts. *Encelia* also presents evidence of this geographic pattern; of the five species that occur on the Baja peninsula, four of them (*E. densifolia*, *E. palmeri*, *E. ventorum* and *E. asperifolia*; Fig. 1) are restricted to the southern portion of the peninsula. Given the crown age of *Encelia*, recent divergences in this genus are most likely to be associated with population movement and isolation spurred by climatic oscillations during the Pleistocene.

Second, although deserts are often characterized as homogeneous swaths of arid land, deserts span large and often steep topological and environmental gradients (Schnitzler *et al.*, 2012; Wiens *et al.*, 2013), which can drive divergent selection and ecological speciation. Although all *Encelia* species are concentrated

in North American deserts, they span multiple such gradients. *Encelia* species live in a diversity of climatic niches, experiencing hottest month temperatures ranging from 25 to 40°C, coldest month temperatures ranging from -5 to 8°C, and driest months ranging from 0 to 5 inches of rain (Figs 3, S9). Although some of these absolute differences are small, they can represent large relative differences when resources are limited. Notably, a few species are climatic outliers such as *E. californica*, which lives along the Californian coast, experiences high rainfall (Figs S9, S10), and *E. actoni*, *E. resinifera* and *E. virginensis*, which all survive freezing temperatures (Figs 3, S10). This climatic variance exemplifies the types of gradients that *Encelia* spans and that can drive diversification and disparification. Unlike species in many rapid radiations (Givnish, 1997), *Encelia* species are rarely sympatric and instead tend to share parapatric boundaries, defined by local environmental and edaphic transitions. Although contemporary geographic distributions do not necessarily reflect historical distributions, this pattern of species turnover across environmental gradients suggests that spatial environmental heterogeneity might have driven *Encelia* speciation.

Third, in arid habitats, multiple environmental gradients can interact and overlap at different spatial scales. Many *Encelia* species have parapatric geographic ranges (Fig. 1) and thus experience very similar climatic conditions (e.g. similar rainfall and solar insolation). However, many of these species pairs are segregated along strong environmental gradients that occur over just a few meters, leading to marked phenotypic differences. Furthermore, the possible anatomical, physiological and phenological adaptations to living in the stressful and resource-limited conditions of deserts are numerous, and combinations of these adaptive traits may all be equally fit, resulting in both high disparification and diversity (Stebbins, 1952; Roddy *et al.*, 2020). For example, *E. ventorum* occurs in sandy dunes that face the ocean, which encroach upon the inland deserts where *E. palmeri* is found (Kyhos *et al.*, 1981; DiVittorio *et al.*, 2020). *Encelia ventorum* can access the water table below the dunes but is also constantly exposed to osmotic stress from ocean spray. Thus, although these two species occur adjacent to each other and experience similar climates, they experience different amounts of water availability and salt stress as well as different soil types, factors that together drive their phenotypic divergence in trichome density, leaf size and shoot hydraulics (Figs 2, 4). Similarly, *E. frutescens* and *E. farinosa* both occur in Death Valley, one of the hottest places in North America. *Encelia farinosa* has large leaves with abundant trichomes, while *E. frutescens* has small leaves with few trichomes (Fig. 3). These differences in leaf morphology influence their microhabitat occupations. *Encelia frutescens* occurs in wash habitats with higher water availability and uses transpirational cooling from its small leaves to maintain low leaf temperatures. In turn, *E. farinosa* occurs along dry slopes where its trichomes reflect solar radiation to maintain low leaf temperatures (Ehleringer, 1988). The same relationships between trichome density, leaf size and water access also seem to influence microhabitat occupation by *E. palmeri* and *E. ventorum* (DiVittorio *et al.*, 2020). These traits might have evolved repeatedly throughout *Encelia* in relation to fine-scale environmental heterogeneity.

These case studies exemplify how no single trait may be responsible for driving the radiation of *Encelia*. Rather, the high lability of multiple traits with compensatory physiological and fitness effects may have enabled rapid trait evolution in *Encelia*, resulting in heightened diversification. As seen in other plant clades, trait lability could be critical in enabling access to a diversity of phenotypes and facilitating diversification within and across environments (Ogburn *et al.*, 2015). Trait lability in combination with multiple equally fit phenotypes would explain the lack of clear correlations between any single trait and broad-scale environmental conditions in *Encelia* (Tables S5, S6; Fig. S12), weak correlations among traits (Fig. S11), and the presence of geographically overlapping species that differ dramatically in morphology (Fig. 4). The diversity of traits associated with desert survival in *Encelia* exemplifies how aridity can be a catalyst of diversification and disparification.

Hybridization and introgression and the *Encelia* radiation

In addition to biogeographic and environmental factors, hybridization and introgression have possibly contributed to the rapid diversification and disparification of *Encelia* by serving as a source of genetic variation and for new species (Anderson & Stebbins, 1954; Stebbins, 1959; Marques *et al.*, 2019). Using two complementary approaches, we found numerous examples of introgression across *Encelia*, including across nonsister species and species in different major clades (Figs S7, S8). In many cases, the instances of introgression are corroborated by field data of naturally occurring hybrids and by cases of suspected hybrid speciation (Fig. 5; Table S5). Rampant hybridization has now been uncovered in multiple rapid radiations, such as the Hawaiian silversword alliance (Barrier *et al.*, 1999), African cichlids (Meier *et al.*, 2017) and *Heliconius* butterflies (Edelman *et al.*, 2019). To this list, we can now add *Encelia*.

Several aspects of *Encelia* biology and geography probably enabled this history of hybridization and introgression. *Encelia* species exhibit few of the barriers that restrict gene flow in other species: all continental species are obligate outcrossers, chromosome number is conserved across the genus, the species are pollinated by generalist pollinators, and, at the regional scale, they have only modest differences in flowering phenology (Ehleringer & Clark, 1988; Clark, 1998). Further, many *Encelia* species ranges are adjacent to each other and map to edaphic transitions (Fig. 1), across which dispersal is more permissible than barriers like mountains. Lastly, in the cold deserts, which are home to a number of species in the *frutescens* clade, midden data suggest that repeated glacial cycles led to repeated range retractions to relictual populations, followed by range expansions (Spaulding & Graumlich, 1986; Thompson & Anderson, 2000). These recurrent bouts of secondary contact could drive introgression between species (Fehlberg & Ranker, 2009; Hewitt, 2011; Folk *et al.*, 2018), as outlined in the species-pump hypothesis (Papadopoulou & Knowles, 2015).

This history of hybridization and introgression might have promoted diversification by helping originate hybrid species. Previous studies of *Encelia* identified four putative cases of hybrid

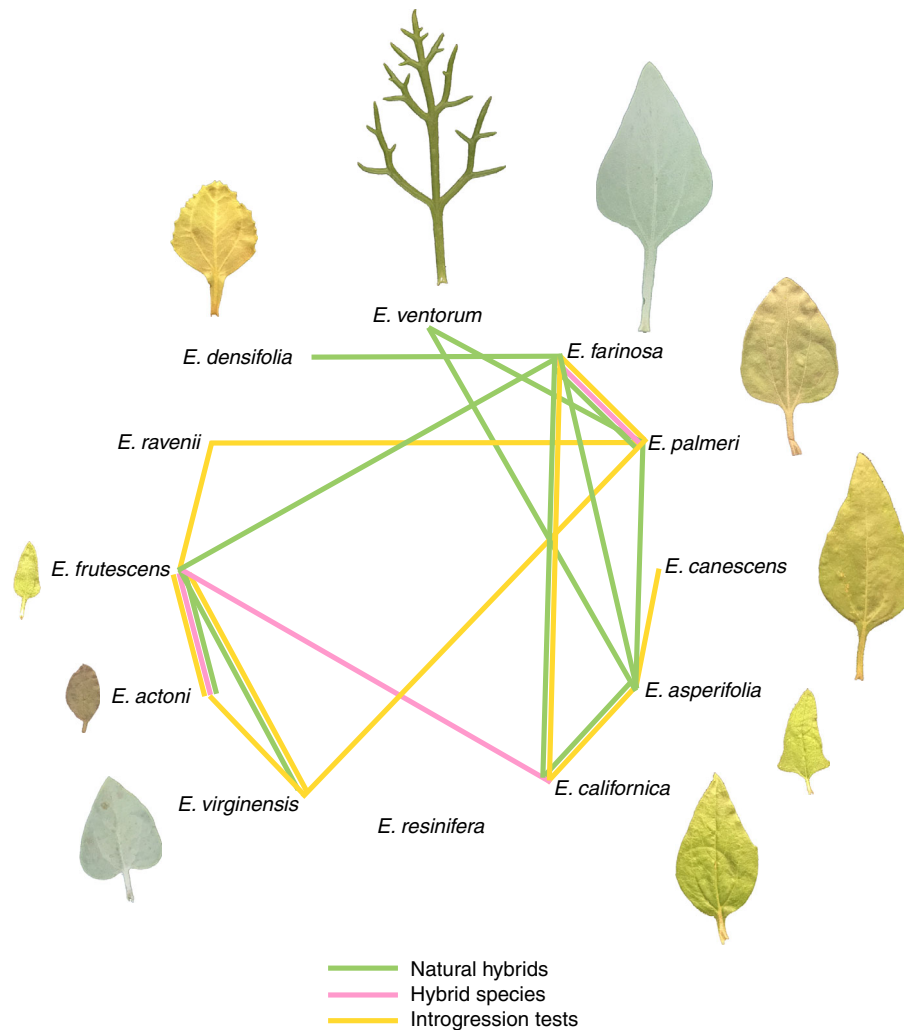


Fig. 5 Hybridization and introgression in *Encelia* based on data from naturally occurring hybrids, putative hybrid species and tests of introgression (D-statistic and SNAQ analyses; Supporting Information Figs S6, S7; Tables S4, S7); lines connect species between which there is evidence of hybridization. In particular, pink lines connect putative parental progenitors of hybrid species; *E. actoni* × *E. frutescens* are hypothesized to have hybridized to form both *E. virginensis* and *E. resinifera*, *E. californica* × *E. frutescens* in *E. asperifolia*, and *E. farinosa* × *E. palmeri* in *E. canescens*. Species are arranged by clade identity and leaf images are relative to size. Hybridization and introgression are rampant across the clade, and many of the species pairs show evidence of hybridization and introgression across multiple measures of introgression.

species (Table S7; Fig. 5): *E. actoni* × *E. frutescens* to result in both *E. virginensis* and *E. resinifera*; *E. californica* × *E. frutescens* to result in *E. asperifolia*; and *E. farinosa* × *E. palmeri* to result in *E. canescens* (Clark & Allan, 1997; Allan *et al.*, 1997; Clark, 1998). As is common in hybrid species (Kadereit, 2015), and as expected by theory (Buerkle *et al.*, 2000), our spatial analyses suggest that these hybrid species occur in disjunct habitats from either progenitor species (Fig. 1). In each of these four cases, our D-statistic and SNAQ results confirm introgression edges either between the parental species or between the parental species and the putative hybrid species. Most notably, the admixture edge from *E. californica* to *E. asperifolia* was estimated at *c.* 50%, as would be expected in hybrid speciation (Fig. S4). Confirming these putative cases of hybrid speciation will require more detailed analyses of the genome and of patterns of reproductive isolation and ecological differentiation between hybrid and parental species (Schumer *et al.*, 2014). Yet, these results provide

preliminary evidence that diversification in *Encelia* could be partially driven by hybrid speciation.

Introgression can also help spur radiations by increasing the amount of genetic variation in a species (Suarez-Gonzalez *et al.*, 2018). Genetic variation can arise from a few sources: *de novo* mutations, standing genetic variation and gene flow between populations or species. Typically, *de novo* mutations are thought unlikely to occur rapidly enough to drive rapid divergence (Barrett & Schluter, 2008). By contrast, both standing genetic variation and gene flow can provide an influx of variation to diverging populations (Hedrick, 2013; Suarez-Gonzalez *et al.*, 2018), allowing them to quickly adapt to new ecological conditions. In either case, distantly related species would exhibit similar phenotypes (Lee & Coop, 2019; Jamie & Meier, 2020), as occurs in *Encelia* (Figs 3, S9). As yet, it is unclear if shared traits in *Encelia* arose from differential sorting of ancestral variation, introgression or true convergent evolution. Reconstructing this history will

require identification of the loci underpinning the trait of interest and characterization of their specific histories (Giska *et al.*, 2019).

Lastly, this history of introgression and hybridization in *Encelia* suggests that the genus might be a syngameon (Clark, 1998), a group of otherwise distinct species interconnected by gene exchange (Lotsy, 1925; Grant, 1971; Hipp *et al.*, 2019). In this scenario, these species can be fully independent evolutionary lineages that retain their cohesiveness and distinctiveness despite hybridization. Species participating in the syngameon can persist as a consequence of reinforcement, assortative mating, divergent selection or selection against hybrids (Cannon & Petit, 2020). In particular, hybrid zone data suggest that extremely strong, divergent selection may be a predominant factor maintaining species boundaries in *Encelia* (DiVittorio *et al.*, 2020). Given that geographically overlapping species are often quite phenotypically divergent (Fig. 4), divergent selection might be helping to maintain species cohesiveness throughout the genus.

Conclusion

Our integrative study within a single desert lineage provides new insights into the processes of plant evolution in one of the harshest terrestrial environments. The evolutionary history of *Encelia* provides an example of a radiation encompassing rapid and recent species formation, high phenotypic disparity and strong ecological divergence – thus meeting many of the key requirements of an adaptive radiation (Givnish, 1997). Across this radiation, ecophenotypic differentiation results in functional and fitness tradeoffs. Rather than homogenizing genetic lineages, interspecific gene flow increases genetic diversity within species and may facilitate adaptation. We suggest that the combined effects of high genetic diversity with high trait lability have enabled access to multiple adaptive peaks, leading to species diversification and disparification across steep environmental gradients at both broad and fine spatial scales. Much remains to be learned about the mechanisms underpinning this radiation. The patchy environmental heterogeneity characteristic of the deserts presents an exciting opportunity to model explicitly the influence of a complex fitness landscape with multiple optima on the genomic background of a radiating lineage (Martin & Richards, 2019). The extent to which interspecific gene flow has enabled adaptation in this scenario is a critical area for continued study.

Acknowledgements







We acknowledge funding from UC MEXUS to CD and SS, a NSF Postdoctoral Fellowship in Biology to SS (DEB-1519732), a CSUDH Norris Faculty Grant to SS, and a postdoctoral fellowship from the Yale Institute for Biospheric Studies to ABR. We thank the UC Riverside AgOps team for their efforts in maintaining the common garden and Danny Eduardo Carvajal López and Darren Sandquist for providing seeds for *E. canescens*. Comments from I. Holmes improved a previous version of this manuscript. MicroCT imaging was performed at the Lawrence Berkeley National Laboratory Advanced Light Source Beamline 8.3.2 microtomography facility, with help from D. Parkinson and A. MacDowell. The

Advanced Light Source is supported by the Director, Office of Science, Office of Basic Energy Services, of the US Department of Energy under contract no. DE-AC01-05CH11231.

Author contributions

SS, ABR and FZ designed the research. SS, ABR, CD, CLH, CRB, AS-A and FZ conducted the research. SS, ABR, SF and FZ analyzed and interpreted data. SS, ABR and FZ wrote the manuscript.

ORCID

Craig R. Brodersen  <https://orcid.org/0000-0002-0924-2570>
Shannon Fehlberg  <https://orcid.org/0000-0002-7386-0832>
Claudia L. Henriquez  <https://orcid.org/0000-0001-7030-5051>
Adam B. Roddy  <https://orcid.org/0000-0002-4423-8729>
Sonal Singhal  <https://orcid.org/0000-0001-5407-5567>
Felipe Zapata  <https://orcid.org/0000-0002-9386-0573>

Data availability

Raw sequence data are available at NCBI BioProject PRJNA691962. Gene trees, alignments, variant call sets, and trait data are available on FigShare at <https://doi.org/10.6084/m9.figshare.13571090.v1>. Scripts used to analyze and visualize data are available on GitHub at: https://github.com/singhal/encelia_phylogeny.

References

- Abramoff MD, Magalhães PJ, Ram SJ. 2004. Image processing with ImageJ. *Biophotonics International* 11: 36–42.
- Ackerly D. 2009. Conservatism and diversification of plant functional traits: evolutionary rates versus phylogenetic signal. *Proceedings of the National Academy of Sciences, USA* 106(Suppl 2): 19699–19706.
- Aiello-Lammens ME, Boria RA, Radosavljevic A, Vilela B, Anderson RP. 2015. spThin: an R package for spatial thinning of species occurrence records for use in ecological niche models. *Ecography* 38: 541–545.
- Allan GJ, Clark C, Rieseberg LH. 1997. Distribution of parental DNA markers in *Encelia virginensis* (Asteraceae: Heliantheae), a diploid species of putative hybrid origin. *Plant Systematics and Evolution* 205: 205–221.
- Anderson E, Stebbins GL. 1954. Hybridization as an evolutionary stimulus. *Evolution* 8: 378–388.
- Arakaki M, Christin P-A, Nyffeler R, Lendel A, Eggli U, Ogburn RM, Spriggs E, Moore MJ, Edwards EJ. 2011. Contemporaneous and recent radiations of the world's major succulent plant lineages. *Proceedings of the National Academy of Sciences, USA* 108: 8379–8384.
- Axelrod DI. 1972. Edaphic aridity as a factor in angiosperm evolution. *American Naturalist* 106: 311–320.
- Baldwin BG, Sanderson MJ. 1998. Age and rate of diversification of the Hawaiian silversword alliance (Compositae). *Proceedings of the National Academy of Sciences, USA* 95: 9402–9406.
- Barrett RDH, Schluter D. 2008. Adaptation from standing genetic variation. *Trends in Ecology & Evolution* 23: 38–44.
- Barrier M, Baldwin BG, Robichaux RH, Purugganan MD. 1999. Interspecific hybrid ancestry of a plant adaptive radiation: allopolyploidy of the Hawaiian silversword alliance (Asteraceae) inferred from floral homeotic gene duplications. *Molecular Biology and Evolution* 16: 1105–1113.

- Bivand R, Rundel C. 2017. *rgeos: interface to geometry engine-open source (GEOS)*. R package v.0.3-26 [WWW document] URL <https://cran.r-project.org/web/packages/rgeos/index.html>.
- Bolger AM, Lohse M, Usadel B. 2014. Trimmomatic: a flexible trimmer for Illumina sequence data. *Bioinformatics* 30: 2114–2120.
- Brodersen CR. 2013. Visualizing wood anatomy in three dimensions with high-resolution X-ray micro-tomography (μ CT) – a review. *IAWA Journal* 34: 408–424.
- Brodersen CR, Roddy AB. 2016. New frontiers in the three-dimensional visualization of plant structure and function. *American Journal of Botany* 103: 184–188.
- Buerkle CA, Morris RJ, Asmussen MA, Rieseberg LH. 2000. The likelihood of homoploid hybrid speciation. *Heredity* 84: 441–451.
- Cannon CH, Petit RJ. 2020. The oak syngameon: more than the sum of its parts. *The New Phytologist* 226: 978–983.
- Chifman J, Kubatko L. 2014. Quartet inference from SNP data under the coalescent model. *Bioinformatics* 30: 3317–3324.
- Clark C. 1998. Phylogeny and adaptation in the *Encelia* Alliance (Asteraceae: Heliantheae). *Aliso: A Journal of Systematic and Evolutionary Botany* 17: 89–98.
- Clark C, Allan GJ. 1997. Hybrid speciation with external barriers: *Encelia* (Asteraceae: Heliantheae), a case study. *American Journal of Botany* 83: 249.
- Conly AG, Brenan JM, Bellon H, Scott SD. 2005. Arc to rift transitional volcanism in the Santa Rosalia region, Baja California Sur, Mexico. *Journal of Volcanology and Geothermal Research* 142: 303–341.
- Crews SC, Hedin M. 2006. Studies of morphological and molecular phylogenetic divergence in spiders (Araneae: Homalonychus) from the American southwest, including divergence along the Baja California Peninsula. *Molecular Phylogenetics and Evolution* 38: 470–487.
- DaCosta JM, Sorenson MD. 2016. ddRAD-seq phylogenetics based on nucleotide, indel, and presence-absence polymorphisms: Analyses of two avian genera with contrasting histories. *Molecular Phylogenetics and Evolution* 94: 122–135.
- DiVittorio CT, Singhal S, Roddy AB, Zapata F, Ackerly DD, Baldwin BG, Brodersen CR, Búrquez A, Fine PVA, Padilla Flores M *et al.* 2020. Natural selection maintains species despite frequent hybridization in the desert shrub *Encelia*. *Proceedings of the National Academy of Sciences, USA* 117: 33373–33383.
- Dolby GA, Bennett SEK, Lira-Noriega A, Wilder BT, Munguía-Vega A. 2015. Assessing the geological and climatic forcing of biodiversity and evolution surrounding the Gulf of California. *Journal of the Southwest* 57: 391–455.
- Durand EY, Patterson N, Reich D, Slatkin M. 2011. Testing for ancient admixture between closely related populations. *Molecular Biology and Evolution* 28: 2239–2252.
- Eaton DAR, Ree RH. 2013. Inferring phylogeny and introgression using RADseq data: an example from flowering plants (*Pedicularis*: Orobanchaceae). *Systematic Biology* 62: 689–706.
- Eaton DAR, Spriggs EL, Park B, Donoghue MJ. 2017. Misconceptions on missing data in RAD-seq phylogenetics with a deep-scale example from flowering plants. *Systematic biology* 66: 399–412.
- Edelman NB, Frandsen PB, Miyagi M, Clavijo B, Davey J, Dikow R, García-Accinelli G, van Belleghem S, Patterson N, Neafsey DE *et al.* 2019. Genomic architecture and introgression shape a butterfly radiation. *Science* 366: 594–599.
- Ehleringer JR. 1988. Comparative ecophysiology of *Encelia farinosa* and *Encelia frutescens*. *Oecologia* 76: 553–561.
- Ehleringer JR, Clark C. 1988. Evolution and adaptation in *Encelia* (Asteraceae). *Plant Evolutionary Biology* 221–248.
- Ehleringer JR, Cook CS. 1987. Leaf hairs in *Encelia* (Asteraceae). *American Journal of Botany* 74: 1532–1540.
- Ehleringer JR, Cook CS. 1990. Characteristics of *Encelia* species differing in leaf reflectance and transpiration rate under common garden conditions. *Oecologia* 82: 484–489.
- Ehleringer J, Mooney HA, Gulmon SL, Rundel PW. 1981. Parallel evolution of leaf pubescence in *Encelia* in coastal deserts of North and South America. *Oecologia* 49: 38–41.
- Ehleringer JR, Sandquist DR. 2018. A tale of ENSO, PDO, and increasing aridity impacts on drought-deciduous shrubs in the Death Valley region. *Oecologia* 187: 879–895.
- Ellis AG, Weis AE, Gaut BS. 2006. Evolutionary radiation of ‘stone plants’ in the genus *Argyroderma* (Aizoaceae): unraveling the effects of landscape, habitat, and flowering time. *Evolution* 60: 39.
- Fehlberg SD, Fehlberg KM. 2017. Spatial genetic structure in brittlebush (*Encelia farinosa*, Asteraceae) in the southwestern deserts of North America: a comparison of nuclear and chloroplast DNA sequences. *Plant Systematics and Evolution* 303: 1367–1382.
- Fehlberg SD, Ranker TA. 2007. Phylogeny and biogeography of *Encelia* (Asteraceae) in the Sonoran and Peninsular deserts based on multiple DNA sequences. *Systematic botany* 32: 692–699.
- Fehlberg SD, Ranker TA. 2009. Evolutionary history and phylogeography of *Encelia farinosa* (Asteraceae) from the Sonoran, Mojave, and Peninsular Deserts. *Molecular Phylogenetics and Evolution* 50: 326–335.
- Fick SE, Hijmans RJ. 2017. WorldClim 2: new 1-km spatial resolution climate surfaces for global land areas. *International Journal of Climatology* 37: 4302–4315.
- Folk RA, Soltis PS, Soltis DE, Guralnick R. 2018. New prospects in the detection and comparative analysis of hybridization in the tree of life. *American Journal of Botany* 105: 364–375.
- Garrick RC, Nason JD, Meadows CA, Dyer RJ. 2009. Not just vicariance: phylogeography of a Sonoran Desert euphorb indicates a major role of range expansion along the Baja peninsula. *Molecular Ecology* 18: 1916–1931.
- GBIF. 10 June 2019. *GBIF occurrence download for encelia*. [WWW document] URL <https://doi.org/10.15468/dl.vu3xn4> [accessed 10 June 2019].
- Giska I, Farelo L, Pimenta J, Seixas FA, Ferreira MS, Marques JP, Miranda I, Letty J, Jenny H, Hackländer K *et al.* 2019. Introgression drives repeated evolution of winter coat color polymorphism in hares. *Proceedings of the National Academy of Sciences, USA* 116: 24150–24156.
- Givnish TJ. 1997. Adaptive radiation and molecular systematics: issues and approaches. In: Givnish TJ, Systma KJ, eds. *Molecular evolution and adaptive radiation*. Cambridge, UK: Cambridge University Press, 1–54.
- Grant V. 1971. *Plant speciation*. New York, NY, USA: Columbia University Press.
- Harmon LJ, Weir JT, Brock CD, Glor RE, Challenger W. 2008. GEIGER: investigating evolutionary radiations. *Bioinformatics* 24: 129–131.
- Hedrick PW. 2013. Adaptive introgression in animals: examples and comparison to new mutation and standing variation as sources of adaptive variation. *Molecular Ecology* 22: 4606–4618.
- Hernández-Hernández T, Brown JW, Schlumpberger BO, Eguiarte LE, Magallón S. 2014. Beyond aridification: multiple explanations for the elevated diversification of cacti in the New World Succulent Biome. *New Phytologist* 202: 1382–1397.
- Hernandez-Hernandez T, Hernandez HM, De-Nova JA, Puente R, Eguiarte LE, Magallon S. 2011. Phylogenetic relationships and evolution of growth form in Cactaceae (Caryophyllales, Eudicotyledoneae). *American Journal of Botany* 98: 44–61.
- Hewitt GM. 2011. Quaternary phylogeography: the roots of hybrid zones. *Genetica* 139: 617–638.
- Hijmans RJ, Van Etten J, Cheng J, Mattiuzzi M, Sumner M, Greenberg JA, Lamigueiro OP, Bevan A, Racine EB, Shortridge A *et al.* 2015. *Package ‘raster’*. [WWW document] URL <https://cran.r-project.org/web/packages/raster/index.html> [accessed 1 June 2019].
- Hipp AL, Whitemore AT, Garner M, Hahn M, Fitzek E, Guichoux E, Cavender-Bares J, Gugger PF, Manos PS, Pearse IS *et al.* 2019. Genomic identity of white oak species in an eastern North American syngameon. *Annals of the Missouri Botanical Garden. Missouri Botanical Garden* 104: 455–477.
- Holt JW, Holt EW, Stock JM. 2000. An age constraint on Gulf of California rifting from the Santa Rosalia basin, Baja California Sur, Mexico. *Geological Society of America Bulletin* 112: 540–549.
- Hughes C, Eastwood R. 2006. Island radiation on a continental scale: exceptional rates of plant diversification after uplift of the Andes. *Proceedings of the National Academy of Sciences, USA* 103: 10334–10339.
- Jamie GA, Meier JJ. 2020. The persistence of polymorphisms across species radiations. *Trends in Ecology & Evolution* 35: 795–808.
- Kadereit JW. 2015. The geography of hybrid speciation in plants. *Taxon* 64: 673–687.

- Klak C, Reeves G, Hedderson T. 2004. Unmatched tempo of evolution in Southern African semi-desert ice plants. *Nature* 427: 63–65.
- Kolb KJ, Sperry JS, Lamont BB. 1996. A method for measuring xylem hydraulic conductance and embolism in entire root and shoot systems. *Journal of Experimental Botany* 47: 1805–1810.
- Kyhos DW. 1967. Natural hybridization between *Encelia* and *Geraea* (Compositae) and some related experimental investigations. *Madroño* 19: 33–43.
- Kyhos DW, Clark C, Thompson WC. 1981. The hybrid nature of *Encelia laciniata* (Compositae: Heliantheae) and control of population composition by post-dispersal selection. *Systematic Botany* 6: 399–411.
- Lee KM, Coop G. 2019. Population genomics perspectives on convergent adaptation. *Philosophical Transactions of the Royal Society of London*. 374: 20180236.
- Li H. 2013. Aligning sequence reads, clone sequences and assembly contigs with BWA-MEM. *arXiv*: 1303.3997 [q-bio.GN].
- Li H, Handsaker B, Wysoker A, Fennell T, Ruan J, Homer N, Marth G, Abecasis G, Durbin R, 1000 Genome Project Data Processing Subgroup. 2009. The sequence alignment/Map format and SAMtools. *Bioinformatics* 25: 2078–2079.
- Liu S, Wei Y, Post WM, Cook RB, Schaefer K, Thornton MM. 2014. NACP MsTMIP. Unified North American Soil Map. ORNL DAAC.
- Lotsy JP. 1925. Species or lineage. *Genetica* 7: 487–506.
- Magallón S, Gómez-Acevedo S, Sánchez-Reyes LL, Hernández-Hernández T. 2015. A metacalibrated time-tree documents the early rise of flowering plant phylogenetic diversity. *New Phytologist* 207: 437–453.
- Magallón S, Sanderson MJ. 2001. Absolute diversification rates in angiosperm clades. *Evolution* 55: 1762–1780.
- Malinsky M, Svardal H, Tyers AM, Miska EA, Genner MJ, Turner GF, Durbin R. 2018. Whole-genome sequences of Malawi cichlids reveal multiple radiations interconnected by gene flow. *Nature Ecology & Evolution* 2: 1940–1955.
- Marques DA, Meier JI, Seehausen O. 2019. A combinatorial view on speciation and adaptive radiation. *Trends in Ecology & Evolution* 34: 531–544.
- Martin CH, Richards EJ. 2019. The paradox behind the pattern of rapid adaptive radiation: how can the speciation process sustain itself through an early burst? *Annual Review of Ecology, Evolution, and Systematics* 50: 569–593.
- Matzke NJ. 2013. Probabilistic historical biogeography: new models for founder-event speciation, imperfect detection, and fossils allow improved accuracy and model-testing. *Frontiers of Biogeography* 5: 242–248.
- Meier JI, Marques DA, Mwaiko S, Wagner CE, Excoffier L, Seehausen O. 2017. Ancient hybridization fuels rapid cichlid fish adaptive radiations. *Nature Communications* 8: 14363.
- Minh BQ, Hahn MW, Lanfear R. 2020. New methods to calculate concordance factors for phylogenomic datasets. *Molecular Biology and Evolution* 37: 2727–2733.
- Mooney H, Zavaleta E. 2016. *Ecosystems of California*. Berkeley, CA, USA: Univ of California Press.
- Niklas KJ. 1994. Morphological evolution through complex domains of fitness. *Proceedings of the National Academy of Sciences, USA* 91: 6772–6779.
- Ogburn RM, Matthew Ogburn R, Edwards EJ. 2015. Life history lability underlies rapid climate niche evolution in the angiosperm clade Montiaceae. *Molecular Phylogenetics and Evolution* 92: 181–192.
- Omernik JM, Griffith GE. 2014. Ecoregions of the conterminous United States: evolution of a hierarchical spatial framework. *Environmental Management* 54: 1249–1266.
- Oskin M, Stock J. 2003. Marine incursion synchronous with plate-boundary localization in the Gulf of California. *Geology* 31: 23–26.
- Pagel M. 1999. Inferring the historical patterns of biological evolution. *Nature* 401: 877–884.
- Papadopoulou A, Knowles LL. 2015. Genomic tests of the species-pump hypothesis: recent island connectivity cycles drive population divergence but not speciation in Caribbean crickets across the Virgin Islands. *Evolution* 69: 1501–1517.
- Paradis E. 2013. Molecular dating of phylogenies by likelihood methods: a comparison of models and a new information criterion. *Molecular phylogenetics and evolution* 67: 436–444.
- Paradis E, Claude J, Strimmer K. 2004. APE: analyses of phylogenetics and evolution in R language. *Bioinformatics* 20: 289–290.
- Pateiro López B, Rodríguez CA. 2010. Generalizing the convex hull of a sample: the R package alphahull. *Journal of Statistical Software* 34: 1–28.
- Peterson BK, Weber JN, Kay EH, Fisher HS, Hoekstra HE. 2012. Double digest RADseq: an inexpensive method for de novo SNP discovery and genotyping in model and non-model species. *PLoS ONE* 7: e37135.
- Pinheiro J. 2009. *nlme: Linear and nonlinear mixed effects models*. R package v. 3.1-96. [WWW document] URL <http://cran.r-project.org/web/packages/nlme/> [accessed 1 June 2019].
- Ree RH, Sanmartín I. 2018. Conceptual and statistical problems with the DEC+J model of founder-event speciation and its comparison with DEC via model selection. *Journal of Biogeography* 45: 741–749.
- Revell LJ. 2012. phytools: an R package for phylogenetic comparative biology (and other things). *Methods in Ecology and Evolution* 3: 217–223.
- Revell LJ, Harrison AS. 2008. PCCA: a program for phylogenetic canonical correlation analysis. *Bioinformatics* 24: 1018–1020.
- Riddle BR, Hafner DJ, Alexander LF, Jaeger JR. 2000. Cryptic vicariance in the historical assembly of a Baja California peninsular desert biota. *Proceedings of the National Academy of Sciences, USA* 97: 14438–14443.
- Roddy AB, van Blerk JJ, Midgley JJ, West AG. 2019. Ramification has little impact on shoot hydraulic efficiency in the sexually dimorphic genus *Leucadendron* (Proteaceae). *PeerJ* 7: e6835.
- Roddy AB, Brodersen CR, Dawson TE. 2016. Hydraulic conductance and the maintenance of water balance in flowers. *Plant, Cell & Environment* 39: 2123–2132.
- Roddy AB, Théroux-Rancourt G, Abbo T, Benedetti JW, Brodersen CR, Castro M, Castro S, Gilbride AB, Jensen B, Jiang G-F *et al.* 2020. The scaling of genome size and cell size limits maximum rates of photosynthesis with implications for ecological strategies. *International Journal of Plant Sciences* 181: 75–87.
- Rognes T, Flouri T, Nichols B, Quince C, Mahé F. 2016. VSEARCH: a versatile open source tool for metagenomics. *PeerJ* 4: e2584.
- Said Gutiérrez-Ortega J, Yamamoto T, Vovides AP, Angel Pérez-Farrera M, Martínez JF, Molina-Freaner F, Watano Y, Kajita T. 2018. Aridification as a driver of biodiversity: a case study for the cycad genus *Dioon* (Zamiaceae). *Annals of Botany* 121: 47–60.
- Sandquist DR. 2014. Plants in Deserts. In: Monson RK, ed. *Yearbook of the United States Department of Agriculture 1911. Ecology and the environment*. New York, NY, USA: Springer, 297–326.
- Sarver BAJ, Keeble S, Cosart T, Tucker PK, Dean MD, Good JM. 2017. Phylogenomic insights into mouse evolution using a pseudoreference approach. *Genome Biology and Evolution* 9: 726–739.
- Schnitzler J, Graham CH, Dormann CF, Schifffers K, Peter LH. 2012. Climatic niche evolution and species diversification in the Cape flora, South Africa (S Higgins, Ed.). *Journal of Biogeography* 39: 2201–2211.
- Schumer M, Rosenthal GG, Andolfatto P. 2014. How common is homoploid hybrid speciation? *Evolution* 68: 1553–1560.
- Smith SA, Brown JW. 2018. Constructing a broadly inclusive seed plant phylogeny. *American Journal of Botany* 105: 302–314.
- Solís-Lemus C, Ané C. 2016. Inferring phylogenetic networks with maximum pseudolikelihood under incomplete lineage sorting. *PLoS Genetics* 12: e1005896.
- Sosa V, Vásquez-Cruz M, Villarreal-Quintanilla JA. 2020. Influence of climate stability on endemism of the vascular plants of the Chihuahuan Desert. *Journal of Arid Environments* 177: 104139.
- Spaulding WG, Graumlich LJ. 1986. The last pluvial climatic episodes in the deserts of southwestern North America. *Nature* 320: 441–444.
- Spotila JA, Farley KA, Sieh K. 1998. Uplift and erosion of the San Bernardino Mountains associated with transpression along the San Andreas fault, California, as constrained by radiogenic helium thermochronometry. *Tectonics* 17: 360–378.
- Stamatakis A. 2014. RAxML version 8: a tool for phylogenetic analysis and post-analysis of large phylogenies. *Bioinformatics* 30: 1312–1313.
- Stebbins GL. 1952. Aridity as a stimulus to plant evolution. *American Naturalist* 86: 33–44.

- Stebbins GL. 1959. The role of hybridization in evolution. *Proceedings of the American Philosophical Society* 103: 231–251.
- Suarez-Gonzalez A, Lexer C, Cronk QCB. 2018. Adaptive introgression: a plant perspective. *Biology Letters* 14: 20170688.
- Thompson RS, Anderson KH. 2000. Biomes of western North America at 18,000, 6000 and 0 ¹⁴C yr BP reconstructed from pollen and packrat midden data. *Journal of Biogeography* 27: 555–584.
- Van Devender TR, Spaulding WG. 1979. Development of vegetation and climate in the southwestern United States. *Science* 204: 701–710.
- Wang Q, Wu S, Su X, Zhang L, Xu X, Lyu L, Cai H, Shrestha N, Liu Y, Wang W *et al.* 2018. Niche conservatism and elevated diversification shape species diversity in drylands: evidence from Zygophyllaceae. *Proceedings of the Royal Society of the Biological Sciences* 285: 20181742.
- Weber MG, Cacho NI, Phan MJQ, Disbrow C, Ramirez SR, Strauss SY. 2018. The evolution of floral signals in relation to range overlap in a clade of California Jewelflowers (*Streptanthus* s.l.). *Evolution* 72: 798–807.
- Wiens JJ, Kozak KH, Silva N. 2013. Diversity and niche evolution along aridity gradients in North American lizards (Phrynosomatidae). *Evolution* 67: 1715–1728.
- Wright IJ, Reich PB, Westoby M, Ackerly DD, Baruch Z, Bongers F, Cavender-Bares J, Chapin T, Cornelissen JHC, Diemer M *et al.* 2004. The worldwide leaf economics spectrum. *Nature* 428: 821–827.
- Yu G, Smith DK, Zhu H, Guan Y, Lam TT. 2017. ggtree: an R package for visualization and annotation of phylogenetic trees with their covariates and other associated data. *Methods in Ecology and Evolution* 8: 28–36.
- Zerbino DR, Birney E. 2008. Velvet: algorithms for *de novo* short read assembly using *de Bruijn* graphs. *Genome Research* 18: 821–829.
- Zhang C, Rabiee M, Sayyari E, Mirarab S. 2018. ASTRAL-III: polynomial time species tree reconstruction from partially resolved gene trees. *BMC Bioinformatics* 19: 153.
- Zhang J, Kobert K, Flouri T, Stamatakis A. 2014. PEAR: a fast and accurate Illumina Paired-End reAd mergeR. *Bioinformatics* 30: 614–620.
- Zizka A, Silvestro D, Andermann T, Azevedo J, Duarte Ritter C, Edler D, Farooq H, Herdean A, Ariza M, Scharn R *et al.* 2019. CoordinateCleaner: standardized cleaning of occurrence records from biological collection databases. *Methods in Ecology and Evolution* 10: 744–751.

Supporting Information

Additional Supporting Information may be found online in the Supporting Information section at the end of the article.

Fig. S1 Effects of model choice and lambda values (λ) on Φ IC (model fit) on chronogram fit to the *Encelia* phylogeny.

Fig. S2 Ancestral range reconstruction in *Encelia* based on the DEC model implemented in BIOGEOBEARS.

Fig. S3 Individual-level phylogenies for *Encelia* inferred using a concatenated maximum-likelihood approach and a coalescent-based approach.

Fig. S4 Nodal support for the individual-level phylogeny for *Encelia* as measured by bootstrap values and site and gene concordance factors.

Fig. S5 Lineage-level phylogenies for *Encelia* inferred using a concatenated maximum-likelihood approach and a coalescent-based approach.

Fig. S6 Effects of missing data on phylogenetic inference in *Encelia*.

Fig. S7 Reconstruction of *Encelia*'s evolutionary history as a network using SNAQ.

Fig. S8 Introgression across *Encelia* as measured by the D-statistic.

Fig. S9 Phenotypic variation in *Encelia*, depicted as phenograms.

Fig. S10 The environmental space occupied by *Encelia* species across climatic variables.

Fig. S11 Pairwise correlations among all measured traits in *Encelia*.

Fig. S12 Correlations between trait and environmental variables in *Encelia*.

Methods S1 Expanded details on how genetic, trait and spatial data were collected and analyzed in this study.

Table S1 Detailed information on the 72 individuals included in this study, including their locality and species designations.

Table S2 Sample sizes for morphological traits and genetic sampling for *Encelia* nominal species and outgroups.

Table S3 The nine morphological and physiological traits measured in this study.

Table S4 Results of significant D-statistic tests for introgression.

Table S5 Global correlations between traits and the environment as inferred from a phylogenetic canonical correlation analysis.

Table S6 Expected correlations between traits and different environmental variables and the results recovered in this study.

Table S7 Instances of hybridization and introgression in the *Encelia* genus from both this study and previously collected data.

Please note: Wiley Blackwell are not responsible for the content or functionality of any Supporting Information supplied by the authors. Any queries (other than missing material) should be directed to the *New Phytologist* Central Office.